



OPEN

The study on the role of O-GlcNAcylation of SIRT3 in regulating mitochondrial oxidative stress during simulate myocardial ischemia-reperfusion

Han Zhou^{1,2}, Yingjie Ji^{1,2}, Jingjie Li¹✉ & Lin Sun¹✉

Myocardial ischemia-reperfusion injury (MIRI) is a significant complication following reperfusion therapy after myocardial infarction. Mitochondrial oxidative stress is a critical factor in MIRI, and Sirtuin 3 (SIRT3), as a major mitochondrial deacetylase, plays a key protective role, with its activity potentially regulated by O-GlcNAcylation. This study used the H9C2 cell line to establish a simulated ischemia/reperfusion (SI/R) model, we utilized co-immunoprecipitated to validate the relationship between O-GlcNAc transferase (OGT) and SIRT3, demonstrated SIRT3 O-GlcNAcylation sites through LC-MS/MS, and performed site mutations using CRISPR/Cas9 technology. The results were validated using immunoblotting. SIRT3 and superoxide dismutase 2 (SOD2) activities were detected using a fluorometric assay, while mitochondrial reactive oxygen species (MROS) levels and cellular apoptosis were assessed using immunofluorescence. We have identified an interaction between SIRT3 and OGT, where SIRT3 undergoes dynamic O-GlcNAcylation at the S190 site, facilitating SIRT3 deacetylase activity. During SI/R, elevated levels of O-GlcNAcylation activate SOD2 by promoting SIRT3 enzyme activity, thereby inhibiting excessive MROS production. This significantly mitigates the occurrence of malignant autophagy in myocardial cells during reperfusion, promoting their survival. Conversely, blocking SIRT3 O-GlcNAcylation at the S190 site exacerbates SI/R injury. We demonstrate that O-GlcNAcylation is a crucial post-translational modification (PTM) of SIRT3 during SI/R, shedding light on a promising mechanism for future therapeutic approaches.

Keywords SI/R, SIRT3, O-GlcNAcylation

Acute myocardial infarction (AMI) is a serious cardiovascular disease that poses a significant threat to human health^{1,2}. Reperfusion therapy is currently the most effective treatment method for reducing ischemic damage³. Unfortunately, myocardial ischemia-reperfusion (MI/R) can lead to additional myocardial injury^{4,5}. Therapeutic strategies aimed at reducing MIRI have been found to be significantly limited in their effectiveness^{6,7}. Targeted reperfusion therapy has been a focal point and bottleneck of research.

Autophagy is believed to play a crucial role in MIRI⁸. Autophagy acts as a protective mechanism during cardiac ischemia by rapidly releasing energy substrates into the cytoplasm, generating ATP through the tricarboxylic acid cycle, thereby reducing cellular metabolic burden and providing energy⁹. Many studies have demonstrated the protective role of autophagy during the ischemic process^{10,11}. However, continuous expression of autophagy during ischemic organ reperfusion may cause damage or even cell death¹²⁻¹⁴. Extensive research has been conducted on the molecular mechanisms of excessive autophagy during myocardial reperfusion. Some studies suggest that excessive MROS generated during reperfusion can significantly induce autophagy and exacerbate myocardial injury¹⁵⁻¹⁷. MROS are primarily degraded by SOD2, whose activity is mainly influenced by its acetylation level¹⁸. SIRT3 is a member of the class III histone deacetylases (HDACs) and is the main deacetylase of mitochondria. SIRT3 regulates the antioxidant enzyme activity of SOD2 through deacetylation¹⁹. Studies have shown that SIRT3 plays a crucial role in cardiac ROS regulation and can thereby modulate autophagy levels

¹Department of Cardiology, The First Affiliated Hospital of Harbin Medical University, Harbin, China. ²These authors contributed equally: Han Zhou and Yingjie Ji. ✉email: lijingjie@hrbmu.edu.cn; drsunlin@sina.com

during reperfusion, alleviating reperfusion injury^{20–22}. Therefore, elucidating the activity regulation mechanism of SIRT3 during MI/R is crucial, yet relevant research remains scarce.

In recent years, O-GlcNAcylation has emerged as a PTM that links changes in cellular metabolism with protein function, becoming a regulatory factor in cardiovascular homeostasis²³. Protein O-GlcNAcylation is a highly dynamic and reversible nutrient-driven process²⁴, controlled by OGT and O-GlcNAcase (OGA), where OGT catalyzes the attachment of a single sugar to target proteins, while OGA reverses this process²⁵. One of the earliest cellular responses to various stresses is a rapid increase in O-GlcNAcylation rates²⁶. Numerous studies have shown that this adaptive increase contributes to enhanced cell survival during MI/R, exerting a protective effect^{27–29}. However, the specific mechanisms remain unclear.

The overlapping roles of SIRT3 and O-GlcNAcylation in MIRI protection have led us to consider the possibility of O-GlcNAcylation modifying SIRT3. In recent years, several members of the Sirtuins family have been found to possess O-GlcNAcylation sites, significantly regulating their activity and involvement in physiological and pathological processes. For instance, SIRT1 is O-GlcNAcylated at Ser 549 at its carboxyl terminus, enhancing its deacetylase activity and protecting cells from stress-induced apoptosis³⁰. Similarly, O-GlcNAcylation modification at Ser 136 of SIRT7 is crucial for maintaining its protein stability and deacetylase ability, and blocking SIRT7 O-GlcNAcylation can delay tumor progression³¹. Therefore, we speculate that SIRT3 may also possess O-GlcNAcylation sites and significantly regulate its deacetylation ability.

In this study, we established an SI/R model to confirm that O-GlcNAcylation of SIRT3 enhances its deacetylase activity, thereby activating SOD2 activity, promoting the degradation of MROS during SI/R, and inhibiting maladaptive autophagy. During SI/R, the loss of SIRT3 O-GlcNAcylation suppresses the SIRT3-SOD2-MROS axis, exacerbating cell apoptosis. These data elucidate a novel molecular mechanism of SIRT3, which may offer new insights and approaches for the clinical treatment of myocardial infarction in the future.

Methods

Cell culture

The cell lines H9C2 were obtained from Procell and cultured in H9C2-specific growth medium (Procell, CM-0089) at 37 °C with 5% carbon dioxide in a cell culture incubator (Thermo). The medium was changed based on the cell growth and adherence status. During medium change, the old medium was first discarded, followed by washing with PBS (Sevenbiotech, SC106) for 2–3 times, and then fresh complete medium was added. If drug stimulation was applied, the drug was added after medium change.

PUGNAC drug intervention

When H9C2 cells reach 80% confluence in the culture flask, PUGNAC (Santa Cruz Biotechnology, sc-204415A; 1.25 µl/ml) is added, and the cells are further cultured for 16 h. For H9C2 cells requiring SI/R treatment, PUGNAC is added to the medium 16 h before ischemia induction. During ischemia, ischemic medium is used instead of regular medium. After ischemia, the medium is switched back to H9C2 cell-specific medium, and PUGNAC is added for an additional 2 h of incubation.

Plasmids

The siRNA-SIRT3 plasmid and siRNA-OGT plasmid were both purchased from Sevenbiotech company. The sequence of siRNA-SIRT3 from 5' to 3' end is GCGUUGUGAAACCUGACAU. The sequence of siRNA-OGT from 5' to 3' end is GCUGAUGCUUAUCCAAUA. The point mutation plasmid (SIRT3^{S190A}) was obtained from FENGHUI Biological Technology company, and plasmid identification was conducted by the same company. According to the manufacturer's instructions, Lipofectamine 3000 (Invitrogen; L3000015) transfection reagent was used for plasmid transfection of H9C2 cells.

Immunoprecipitation (IP) and CoIP

Collect the cells and add cell lysis buffer containing RIPA buffer (Beyotime Biotechnology; P0013B), phosphatase inhibitors (Beyotime Biotechnology; P1045), and PMSF (Beyotime Biotechnology; ST505). Incubate with respective protein antibodies by vertical rotation at 4 °C overnight. Add protein A + G agarose beads (Santa Cruz Biotech; sc-2003) and continue shaking for 8 h. Collect the precipitate and add 5 × loading buffer (Beyotime Biotechnology; P0015) for protein denaturation (100 °C, 10 min). Centrifuge to collect the supernatant and store the samples at –80 °C for subsequent analysis.

SI/R model

H9c2 cells were exposed to ischemia by replacing H9C2-specific growth medium with ischemic buffer (pH 6.3), which contained 137 mM NaCl, 15.8 mM KCl, 0.49 mM MgCl₂, 0.9 mM CaCl₂, 4 mM HEPES, 10 mM 2-deoxyglucose, 20 mM sodium lactate and 1 mM sodium dithionite. Subsequently, cells were incubated in a self-made sealing box in an atmosphere of 95% nitrogen and 5% CO₂ at 37 °C for 4 h. Following ischemia, reperfusion was initiated by incubating in H9C2-specific growth medium at 37 °C with 5% CO₂ for a further 2 h.

O-GlcNAc site mapping of SIRT3

This experiment was conducted by Beijing BiotechPack company to analyze the PTMs of SIRT3 protein in H9C2 cells (Project No.: BTP-20230804-07). Firstly, proteins were extracted from the samples, followed by CO-IP and subsequent trypsin digestion. The processed samples were then subjected to liquid chromatography-tandem mass spectrometry (LC-MS/MS) analysis to obtain raw mass spectrometry data files. The data were analyzed using the Byonic software to match and identify the results.

Western blotting

The cells were lysed thoroughly using cell lysis buffer. If mitochondrial proteins (SIRT3) needed to be collected, the cell lysate was sonicated for 10 min using an ultrasonic cell disruptor (Thermo) before the lysis process. The supernatant was collected after centrifugation, and 5× loading buffer was added for protein denaturation. Subsequently, SDS-PAGE gel separation was performed, followed by the transfer of proteins onto a polyvinylidene difluoride (PVDF) membrane. The primary antibody data is presented in Supplementary Table 1.

SIRT3 and SOD2 activity assay

SIRT3 deacetylase activity was measured with a SIRT3 Direct Fluorescent Screening Assay Kit (Cayman; 10011566). SOD2 activity was measured with a SOD activity assay kit (Boxbio; AKAO001M) according to the manufacturer's protocol.

TUNEL assay

Using a One-Step TUNEL Apoptosis Assay Kit (Beyotime Biotechnology; C1088), cells were fixed with an immunostaining fixative solution (Beyotime Biotechnology; P0098) for 30 min. Immunostaining permeabilization buffer (Beyotime Biotechnology; P0097) was then added and incubated for 5 min. Subsequently, 100 µl of TUNEL staining solution was added to the samples and incubated in the dark for 60 min. The samples were then sealed with an antifade mounting medium (Beyotime Biotechnology; P0126) and observed under a fluorescence microscope.

MROS detection

MROS was measured using the Mitochondrial ROS Detection Assay Kit (Cayman; 701600). Each well was incubated with 100 µL of pre-warmed Mitochondrial ROS Detection Reagent staining solution at 37 °C in the dark for 20 min. For the positive control, antimycin A working solution was added to the designated wells at a concentration of 8 µM and incubated at 37 °C for 1 h. Fluorescence was read under a fluorescence microscope with an excitation wavelength of 480–515 nm and an emission wavelength of 560–600 nm.

Statistical analysis

The data are shown as the means ± SD. We used the Shapiro–Wilk test to analyze the normality of the data. For comparisons between two groups, statistical analysis was performed using an unpaired t-test. For multiple group comparisons, the Brown–Forsythe and Welch ANOVA tests were used. A value of $P < 0.05$ was statistically significant. All statistical analyses were performed using GraphPad Prism Version 7.0 (GraphPad Prism Software).

Results

OGT can interact with SIRT3

Since OGT is the sole enzyme responsible for protein O-GlcNAcylation within cells, we initially investigated whether OGT could interact with SIRT3 to assess potential associations between O-GlcNAcylation and SIRT3. H9C2 cell extracts were CoIP with anti-SIRT3 antibody or control immunoglobulin (IgG). As anticipated, immunoblot analysis revealed a prominent detection of OGT in the immunoprecipitates obtained with anti-SIRT3 antibody, whereas no OGT was detected in the control antibody group (Fig. 1a). To confirm the specificity of the SIRT3 antibody, SIRT3 expression in H9C2 cells was silenced using SIRT3-specific siRNA. OGT was barely detected in the CoIP from SIRT3-silenced cells (Fig. 1a). Additionally, reciprocal CoIP experiments were

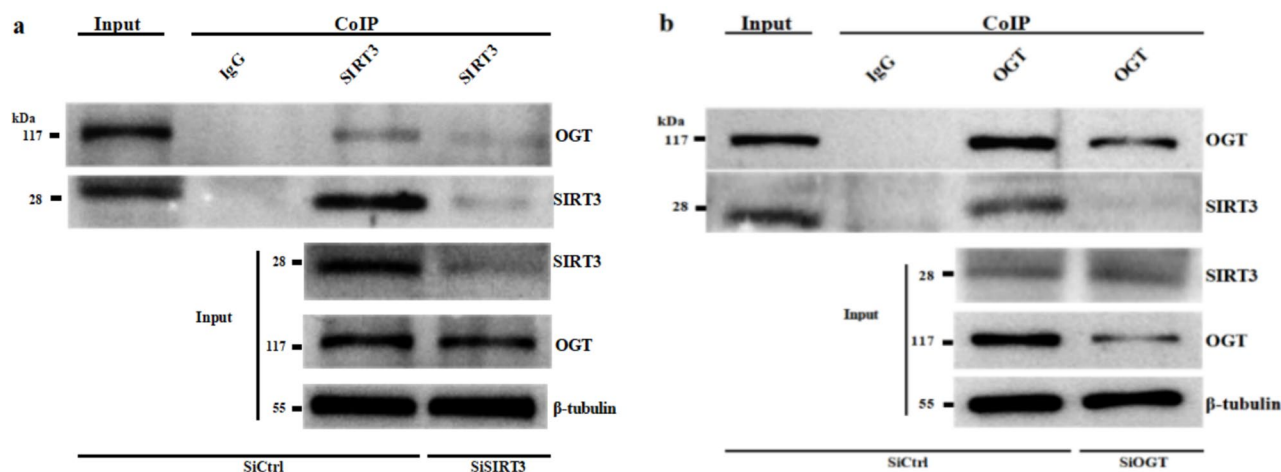


Fig. 1. (a) Using SIRT3-silenced H9C2 cells as the negative control, immunoblotting was employed to examine whole-cell lysates (input), immunoprecipitates with anti-SIRT3 antibody, and control immunoglobulins ($n = 3$). (b) Immunoblotting was utilized to compare the CoIP induced by anti-OGT antibody in whole-cell lysates of control and OGT-silenced H9C2 cells ($n = 3$). siCtrl: Non-targeting plasmid; siOGT: OGT silenced; siSIRT3: SIRT3 silenced.

performed, as depicted in Fig. 1b, showing that SIRT3 could also be CoIP with OGT-specific antibody, and OGT silenced significantly abolished the CoIP of SIRT3.

SIRT3 is O-GlcNAcylated at Serine 190

CoIP results indicate that SIRT3 can interact with OGT, suggesting a potential presence of O-GlcNAcylation modification on SIRT3. To determine the precise site of O-GlcNAcylation, LC-MS/MS analysis was performed. O-GlcNAcylation was localized to Serine 190 (S190) within the peptide region 184–191 of SIRT3 (Fig. 2a). Comparison of the S190 O-GlcNAcylation site of rat SIRT3 with the corresponding region in other mammals revealed a high degree of conservation (Fig. 2b). These findings suggest that SIRT3 O-GlcNAcylation may be highly conserved throughout mammalian evolution.

To validate whether SIRT3 primarily undergoes O-GlcNAcylation at this site, we constructed a single-point mutation plasmid in which SIRT3 Serine 190 was mutated to Alanine (S190A) for subsequent studies. CoIP results showed that SIRT3 could undergo O-GlcNAcylation and the O-GlcNAcylation of SIRT3 significantly decrease significantly in S190A group compared with WT (Fig. 2c). Simultaneously, treatment of H9C2 cells with the OGA inhibitor PUGNAC significantly promoted O-GlcNAcylation of SIRT3 in the WT group and had a certain impact on the S190A group (Fig. 2c). However, statistical analysis indicated that this impact was more significant in the WT group (Fig. 2d), indicating that O-GlcNAcylation at S190 is highly dynamic. These results suggest that S190 is the primary O-GlcNAcylation site of SIRT3.

The O-GlcNAcylation of SIRT3 at S190 can enhance its deacetylase activity

To investigate the effect of O-GlcNAcylation on SIRT3 deacetylase activity, we measured the activity of SIRT3 in H9C2 cells after different treatments using a SIRT3 activity assay kit. We first assessed the O-GlcNAcylation levels in each group (Fig. 3a), and the results showed that the O-GlcNAcylation level in the S190A group was significantly lower than that in the WT group ($P < 0.01$), while PUGNAC treatment significantly increased the O-GlcNAcylation level in the WT group ($P < 0.05$), with no significant effect on the S190A group ($P > 0.05$) (Fig. 3b). Next, we characterized the activity of SIRT3 in each group by fluorescence intensity. Compared with the WT group, the SIRT3 enzyme activity decreased in the S190A group ($P < 0.001$), while PUGNAC treatment significantly enhanced the activity of SIRT3 in the WT group ($P < 0.0001$), with no significant effect on the S190A group ($P > 0.05$) (Fig. 3c). These results indicate that O-GlcNAcylation of SIRT3 at S190 significantly enhances SIRT3 deacetylase activity.

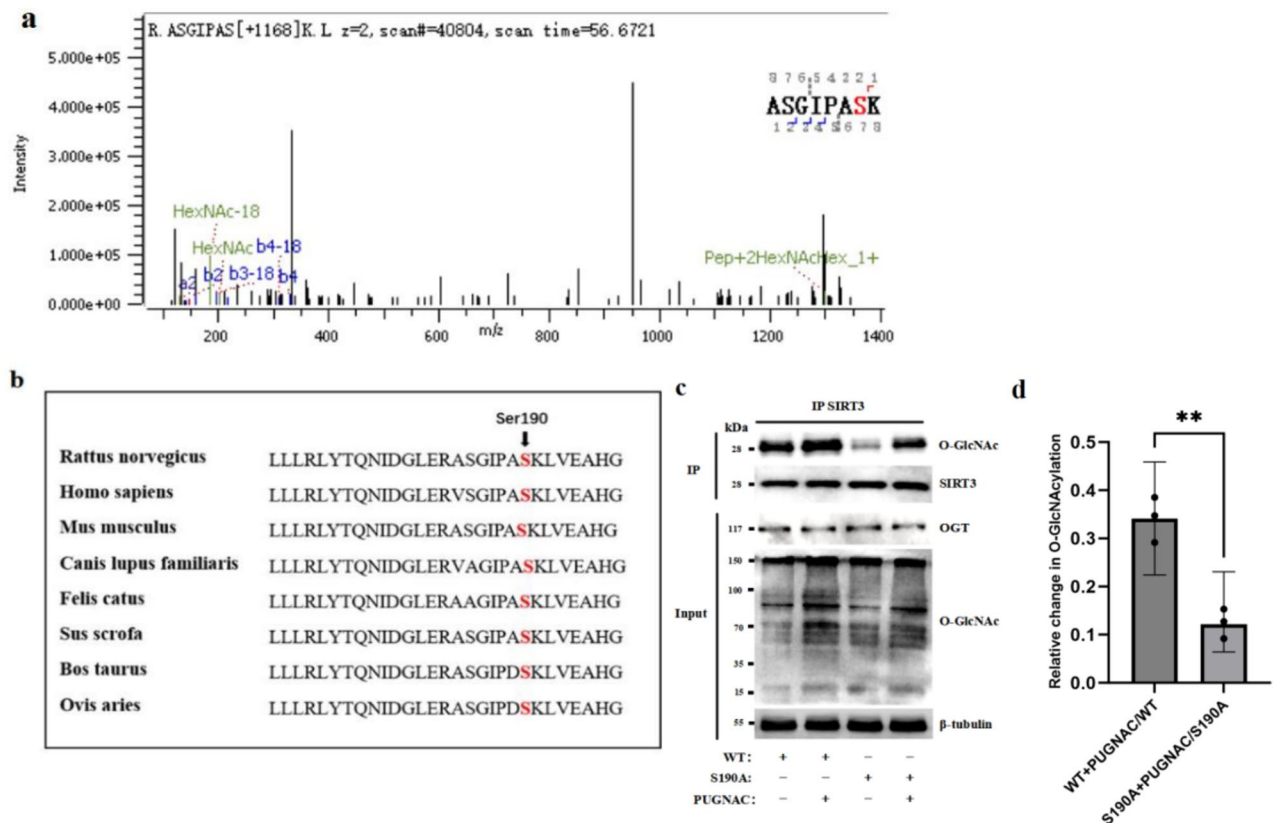


Fig. 2. (a) LC-MS/MS detected the O-GlcNAcylation peptide of SIRT3(184–191). (b) Comparison of the S190 site of rat SIRT3 with the corresponding region in other mammals. (c) Verification of the O-GlcNAcylation of the SIRT3 S190 site using PUGNAC and point mutation plasmids ($n = 3$). (d) Comparison of O-GlcNAcylation changes after the addition of PUGNAC in WT and S190A groups. ($n = 3$).

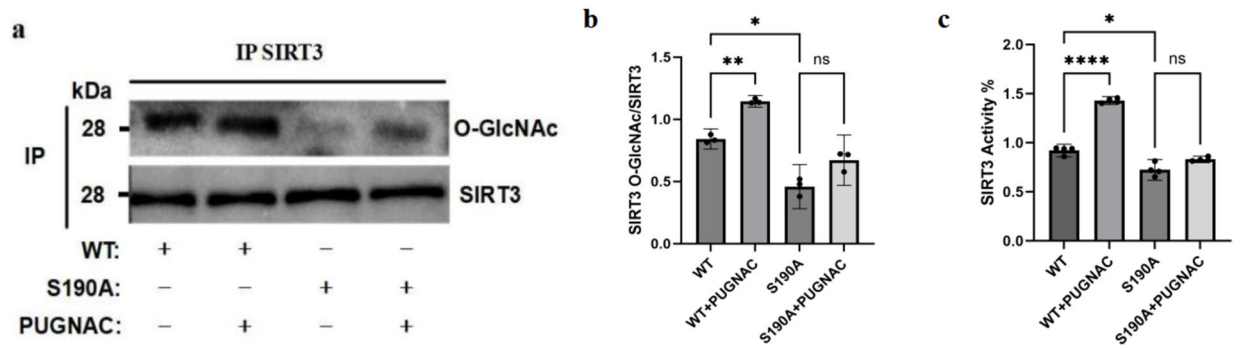


Fig. 3. (a) Validation of changes in SIRT3 O-GlcNAcylation levels using point mutation plasmids and PUGNAC. (b) Statistical graphs obtained by calculating the corresponding results (n=3). (c) Statistical graphs of changes in SIRT3 enzymatic activity in each group detected using point mutation plasmids and PUGNAC (n=3). (* $P < 0.05$; ** $P < 0.01$; *** $P < 0.001$; **** $P < 0.0001$).

SI/R activates SIRT3 by upregulating the O-GlcNAcylation in H9C2 cells

We conducted in vitro studies using H9C2 cells to SI/R according to previously established methods³², to investigate whether SIRT3 is activated by upregulating myocardial cell O-GlcNAcylation levels under SI/R conditions. First, we recorded the temporal changes in O-GlcNAcylation levels in H9C2 cells during the SI/R process.. We standardized the ischemia time to 4 h. During the first hour of reperfusion, O-GlcNAcylation levels were significantly elevated, reaching a peak at the second hour of reperfusion, and then slowly returned to baseline levels (Fig. 4a,b). Therefore, we selected the 2 h reperfusion time point for further study.

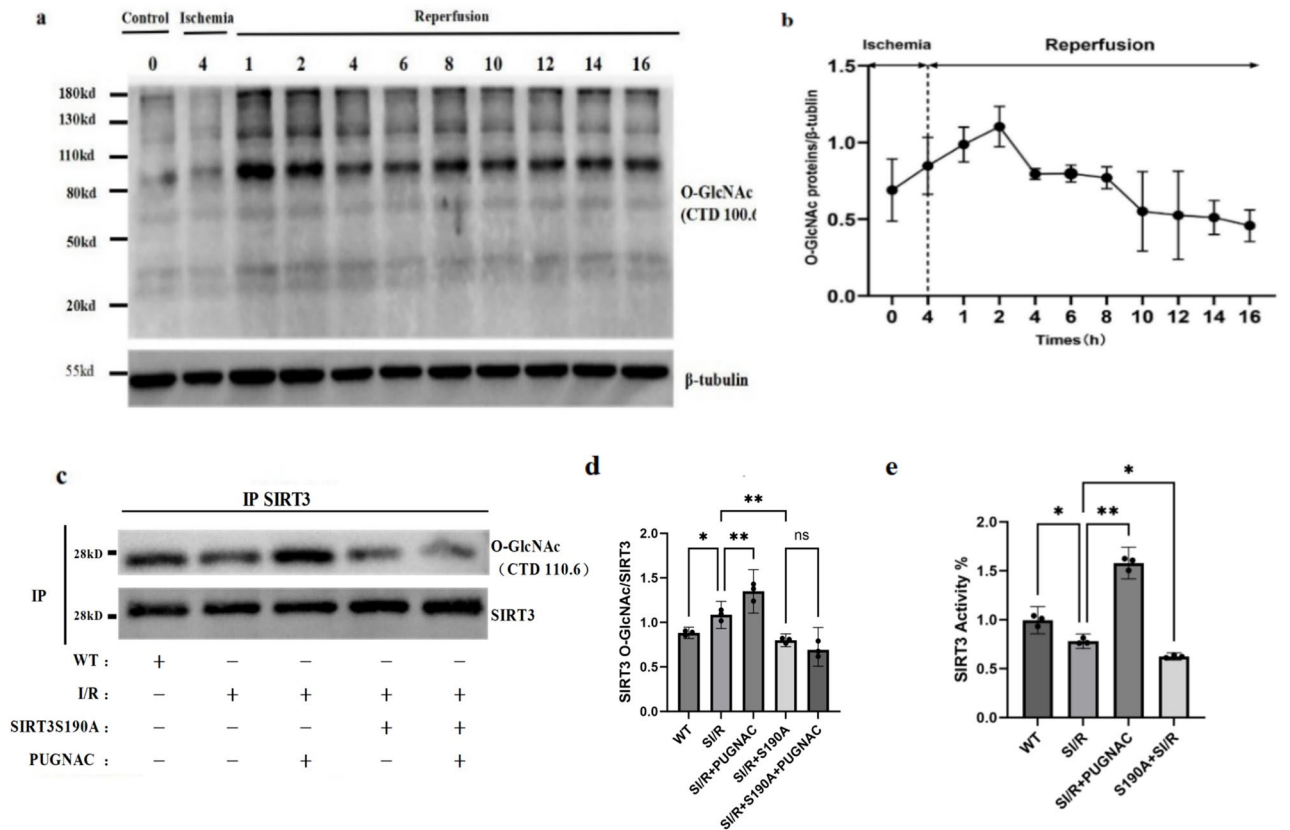


Fig. 4. (a) The trend of SIRT3 O-GlcNAcylation levels with the duration of SI/R, with an ischemic time of 4 h and reperfusion times at 0 h, 1 h, 2 h, 4 h, 8 h, 10 h, 12 h, 14 h, and 16 h. (b) Statistical graphs obtained by calculating the corresponding time curve results (n=3). (c) Detection of changes in SIRT3 O-GlcNAcylation levels in each group using point mutation plasmids and PUGNAC. (d) Statistical graphs obtained by calculating the corresponding results from (c) (n=3). (e) Statistical graphs of changes in SIRT3 enzymatic activity in each group detected using point mutation plasmids and PUGNAC (n=3). (* $P < 0.05$; ** $P < 0.01$; *** $P < 0.001$; **** $P < 0.0001$).

Compared with the WT group, the SI/R group exhibited an upregulation in O-GlcNAcylation levels ($P < 0.01$) (Fig. 4c,d), but SIRT3 activity showed a slight decrease ($P < 0.01$) (Fig. 4e). Interestingly, we observed a further significant decrease in SIRT3 activity in the S190A + SI/R group compared with the SI/R group alone ($P < 0.05$) (Fig. 4e). Additionally, the O-GlcNAcylation levels of SIRT3 in the S190A + SI/R group were significantly lower than those in the SI/R group ($P < 0.01$) (Fig. 4c,d), suggesting that O-GlcNAcylation may be a key factor promoting SIRT3 activity under SI/R conditions. To further validate this notion, we treated cells after SI/R with PUGNAC. The PUGNAC + SI/R group showed a significant increase in SIRT3 O-GlcNAcylation levels ($P < 0.05$) (Fig. 4c,d) as well as SIRT3 enzyme activity ($P < 0.0001$) (Fig. 4e) compared with the SI/R group. These results indicate that O-GlcNAcylation dynamically positively regulates SIRT3 activation during SI/R, and O-GlcNAcylation of SIRT3 enhances its deacetylase activity under SI/R conditions.

O-GlcNAcylation of SIRT3 can inhibit SI/R-induced cellular autophagy

Existing research suggests that SIRT3 regulates MROS by deacetylating SOD2, thereby modulating autophagy levels. Based on our results which we found that O-GlcNAcylation can enhance SIRT3 activity, we hypothesized that the upregulation of SIRT3 O-GlcNAcylation levels may inhibit SI/R-induced autophagy. Firstly, we examined the acetylation levels of SOD2 in each group (Fig. 5a), SOD2 activity (Fig. 5c), and MROS levels (Fig. 5d). We found that compared with the WT group, the SI/R group exhibited decreased SOD2 activity ($P < 0.0001$), increased acetylation levels ($P < 0.05$), and corresponding elevation in MROS levels ($P < 0.01$). Additionally, in the S190A + SI/R group, SOD2 activity was further decreased compared with the SI/R group ($P < 0.01$), acetylation levels were further elevated ($P < 0.01$), and MROS levels were significantly increased ($P < 0.0001$) (Fig. 5b,c,e). This suggests that the level of SIRT3 O-GlcNAcylation may regulate an active axis such as SIRT3-SOD2-MROS. Furthermore, when we treated the SI/R group with PUGNAC, we found that the SOD2 activity in the PUGNAC + SI/R group was higher compared with the SI/R group ($P < 0.0001$), with lower acetylation levels ($P < 0.05$), and a corresponding decrease in MROS levels ($P < 0.05$) (Fig. 5b,c,e). These results correspond to the previous SIRT3 activity results (Fig. 4e). To exclude the potential impact of the PUGNAC drug itself on the experiments, we found that the SOD2 activity and SOD2 acetylation levels in the PUGNAC + S190A + SI/R group were like those in the S190A + SI/R group ($P > 0.05$) (Fig. 5b,c). Interestingly, we found that the intervention of the PUGNAC drug had a suppressive effect on the MROS levels in both the SI/R group and the S190 + SI/R group. However, the inhibitory effect of PUGNAC on the S190 + SI/R group was significantly weaker than that on the SI/R group ($P < 0.0001$) (Fig. 5e).

This may be attributed to the regulation of MROS by other mechanisms as well. However, it is undeniable that SOD2 is one of the most significant antioxidant enzymes. This further supports the notion that O-GlcNAcylation of SIRT3 can reduce MROS generation by upregulating SOD2 activity.

Next, we investigated whether O-GlcNAcylation of SIRT3 could inhibit SI/R-induced MROS-related autophagy (Fig. 5f). We found that compared with the WT group, the SI/R group exhibited an upregulation in the autophagy-related protein Lc3II/Lc3I levels ($P < 0.05$). Furthermore, the S190A + SI/R group showed a further significant increase in autophagy levels ($P < 0.05$), while the PUGNAC + SI/R group showed no significant difference in autophagy levels compared with the SI/R group ($P > 0.05$) (Fig. 5g). We speculate that this may be due to the lack of sufficient sample size resulting in non-significant differences. Similarly, the PUGNAC + S190A + SI/R group showed a trend of decreased autophagy levels compared with the S190A + SI/R group, but no significant difference was observed ($P > 0.05$). However, it is noteworthy that the protective effect of PUGNAC on the SI/R group was significantly superior to that of the S190A + SI/R group ($P < 0.05$) (Fig. 5g). These results indicate that O-GlcNAcylation of SIRT3 can inhibit SI/R-induced autophagy.

O-GlcNAcylation of SIRT3 can reduce the rate of cell apoptosis after SI/R injury

We used the TUNEL assay to detect apoptosis in H9C2 cells after different treatments (Fig. 6a). As expected, compared with the WT group, SI/R treatment resulted in increased apoptosis in H9C2 cells ($P < 0.01$), while cells in the S190A + SI/R group were more prone to cell death ($P < 0.0001$) (Fig. 6b). More importantly, PUGNAC treatment significantly protected SI/R cells from death ($P < 0.05$), but its effect on S190A + SI/R was relatively weaker ($P < 0.0001$) (Fig. 6b). In summary, O-GlcNAcylation of SIRT3 can to some extent protect myocardial cells from SI/R injury.

Discussion

This experiment contributes to two main aspects: Firstly, through mass spectrometry analysis, it was clearly demonstrated that SIRT3 protein can undergo O-GlcNAcylation. Additionally, S190 was identified as the site of O-GlcNAcylation in rat cardiomyocyte SIRT3, establishing a pivotal foundation for future scientific investigations. Secondly, employing a cell-based SI/R model, we elucidated the critical protective mechanism of O-GlcNAcylation in myocardial cells during the pathological process of I/R. Specifically, O-GlcNAcylation of SIRT3 activated its deacetylase activity, subsequently activating the SIRT3-SOD2-MROS axis, mitigating the early accumulation of MROS during reperfusion, inhibiting cellular autophagy, and reducing SI/R injury (Fig. 7). Furthermore, we elucidated for the first time the relationship between O-GlcNAcylation and cellular autophagy in the pathological process of SI/R, thus paving the way for novel approaches in the reperfusion therapy of coronary heart disease.

SIRT3 is highly expressed in tissues with high metabolic rates, such as the mitochondria of the heart and brain, where it serves as the primary deacetylase of acetyl-lysine residues, playing crucial roles in various physiological and pathological processes in the heart^{33,34}. Recently, PTMs of SIRT3 have become a focus of research interest. For instance, SIRT3 can undergo phosphorylation, and phosphorylation of SIRT3 at Thr150/Ser159 mediated by Cyclin B1-CDK1 in mitochondria further enhances its enzymatic activity, potentially serving as an effective

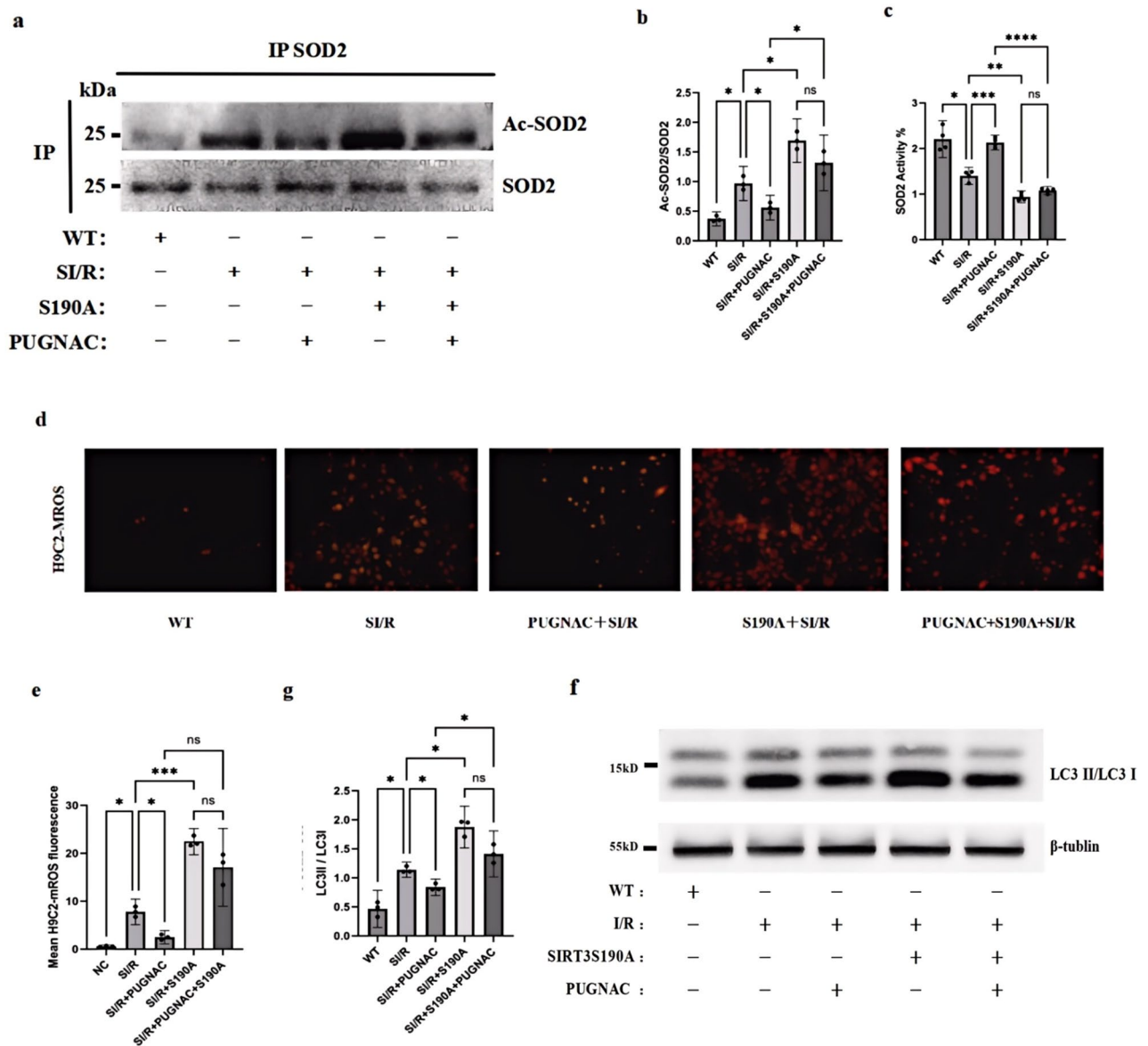


Fig. 5. (a) Detection of changes in SOD2 and Ac-SOD2 levels in each group using point mutation plasmids and PUGNAC. (b) Statistical graphs obtained by calculating the corresponding results from (a) ($n=3$). (c) Detection of changes in SOD2 enzymatic activity in each group using point mutation plasmids and PUGNAC ($n=3$). (d) Fluorescence images of MROS changes in each group detected using point mutation plasmids and PUGNAC. (e) Statistical graphs obtained by calculating the corresponding results from (d) ($n=3$). (f) Detection of trends in LC3II and LC3I protein levels in each group using point mutation plasmids and PUGNAC, along with the assessment of β -tubulin differences in each group. (g) Statistical graphs obtained by calculating the corresponding results from (f) ($n=4$). (* $P<0.05$; ** $P<0.01$; *** $P<0.001$; **** $P<0.0001$).

target for inhibiting tumor growth through radiotherapy³⁵. Additionally, SIRT3 has been found to undergo SUMOylation, with SUMOylation inhibiting its catalytic activity. During fasting in mice, SENP1 activates SIRT3 deacetylase activity by deSUMOylating SIRT3, promoting fatty acid oxidation and energy utilization, thereby controlling mitochondrial metabolic responses to stress³⁶. These findings underscore the critical importance of PTMs in regulating the activity of SIRT3 under stress conditions. O-GlcNAcylation is a pivotal PTM that contributes to the regulation of various biological functions, including the cell cycle, transcription and translation, mitochondrial function, and protein synthesis^{23,37}. Recently, members of the Sirtuin family have been discovered to possess O-GlcNAcylation sites, significantly modulating their activity and involvement in physiological and pathological processes, such as SIRT1³⁰ and SIRT7³¹. The Sirtuin family proteins are highly conserved NAD⁺-dependent deacetylases³⁸. Given the consistent protective roles of SIRT3 and O-GlcNAc in MIRI it is plausible to speculate that SIRT3 also harbors O-GlcNAcylation sites and significantly regulates its deacetylation activity.

Our study investigated the role of O-GlcNAcylation modification of SIRT3 in mediating MIRI response. Through CoIP, we found that SIRT3 interacts with OGT. Mass spectrometry analysis led us to identify S190 as a potential primary regulatory O-GlcNAcylation site, which, upon comparison with other mammals, showed high

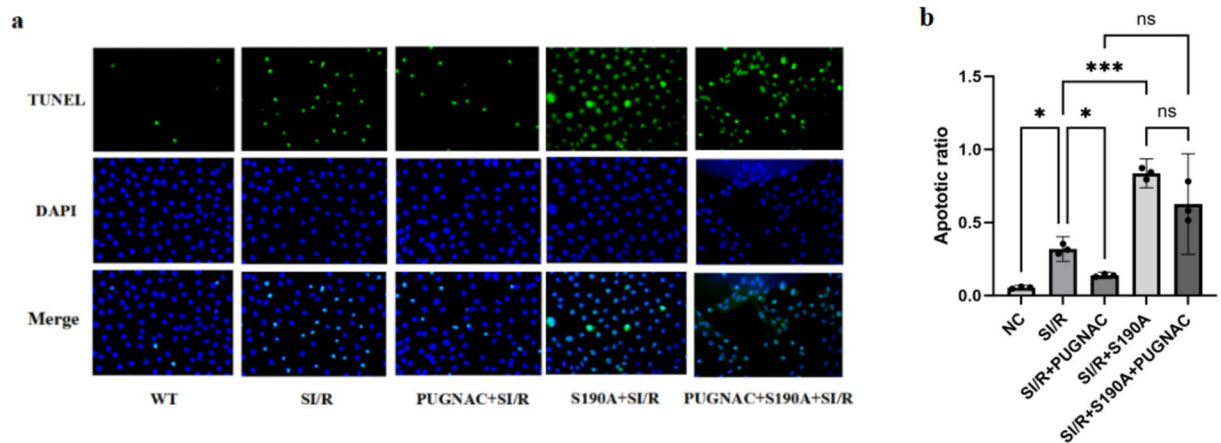


Fig. 6. (a) Detection of cellular apoptosis levels in each group using the TUNEL assay. (b) Statistical graphs obtained by calculating the corresponding results from (a) ($n=3$). (* $P<0.05$; ** $P<0.01$; *** $P<0.001$; **** $P<0.0001$).

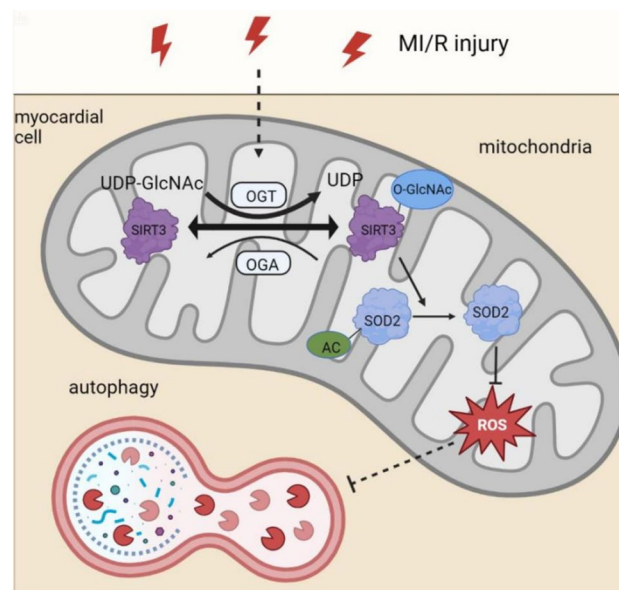


Fig. 7. Schematic diagram illustrating the potential mechanism of the protective effect of SIRT3 O-GlcNAcylation against MIRI.

conservation. Using plasmid technology, we mutated the serine residue at this site to alanine (S190A), resulting in a significant decrease in SIRT3 O-GlcNAcylation levels, accompanied by a decline in SIRT3 activity. Additionally, the OGA inhibitor PUGNAC showed no significant rescue effect on this change, indicating that S190 is the main O-GlcNAcylation site of SIRT3, and O-GlcNAcylation at S190 significantly enhances SIRT3 deacetylase activity. Consistent with other studies, we found that overall O-GlcNAcylation levels were significantly upregulated during SI/R. We attempted to determine whether this upregulation of O-GlcNAcylation could activate SIRT3. We first measured the time course of O-GlcNAcylation levels in H9C2 cells under SI/R conditions and found that SIRT3 O-GlcNAcylation levels peaked at 2 h of reperfusion, prompting us to select the 2 h reperfusion time point for subsequent experiments. We found that the level of SIRT3 O-GlcNAcylation increased during the SI/R process, but the activity of SIRT3 decreased, which seems to be inconsistent with our previous experimental results. We believe that this may be due to the interference with SIRT3 activity by other inhibitory factors during SI/R in addition to O-GlcNAcylation. For instance, studies have shown that following SI/R in H9C2 cells, the expression of AMP-activated protein kinase (AMPK) decreases. AMPK can directly bind to and activate SIRT3, so its downregulation can lead to a reduction in SIRT3 activity³⁹. Additionally, during SI/R in H9C2 cells, SIRT3 activity is regulated by melatonin membrane receptor 2 (MT2), which leads to its reduction. Exogenous melatonin administration can rescue this process⁴⁰. Therefore, although O-GlcNAcylation levels increase after SI/R, this may not be sufficient to prevent the decline in SIRT3 activity, and higher levels of O-GlcNAcylation may be needed to rescue it. However, after adding PUGNAC to further enhance SIRT3 O-GlcNAcylation, we found a significant increase in SIRT3 activity, which is consistent with our speculation. Meanwhile, we found

that the SIRT3 activity in the S190A + SI/R group was further reduced compared to the SI/R group, which led to an elevation in SOD2 acetylation levels, a reduction in SOD2 activity, and exacerbated production of MROS and subsequent oxidative stress-related malignant autophagy. TUNEL staining showed that the death rate of H9C2 cells in the S190A group was significantly higher than that in the control group under SI/R conditions. Therefore, we conclude that SIRT3 O-GlcNAcylation reduces oxidative stress damage and malignant autophagy through the SOD2-MROS axis, exerting a significant protective effect during SI/R.

In recent years, autophagy has been recognized as a key process in maintaining normal cardiac structure and function⁸. Autophagy plays a dual role in MIRI. During cardiac ischemia, autophagy is considered a protective mechanism, with many studies demonstrating its protective effects during ischemia^{10,11}. However, when organs experience reperfusion, the sustained expression of autophagy may cause cellular damage and even lead to cell death¹². Our study indicates that O-GlcNAcylation reduces myocardial autophagic cell death through the SIRT3-SOD2 pathway dependency. However, the potential myocardial protective mechanisms of O-GlcNAcylation remain largely unknown. For instance, some studies suggest that O-GlcNAcylation may exert protective effects during I/R by alleviating calcium overload⁴¹. Other research suggests that O-GlcNAcylation protects against I/R injury by attenuating the opening of the mitochondrial permeability transition pore (MPTP)⁴². Additionally, O-GlcNAcylation seems to be involved in reducing endoplasmic reticulum stress-induced damage by weakening CHOP induction⁴³. Hence, the potential endogenous protective mechanisms of O-GlcNAcylation, especially in MIRI, warrant further investigation.

Conclusions

In summary, our study revealed that SIRT3 protein undergoes O-GlcNAcylation, and we confirmed S190 as the site of O-GlcNAcylation in rat cardiomyocytes. We demonstrated that O-GlcNAcylation increases SIRT3 deacetylase activity, thereby activating the SIRT3-SOD2-MROS axis, reducing the excessive accumulation of early reperfusion MROS, and inhibiting cellular autophagy levels, thereby reducing reperfusion injury. Our findings elucidate the myocardial protective mechanism triggered by O-GlcNAcylation, providing potential insights for identifying new therapeutic targets to prevent MI/R and slow the progression of heart failure.

Limitation

Firstly, this study used H9C2 cell SI/R and did not conduct in vivo whole heart experiments. Secondly, due to the lack of a cell culture incubator with relevant conditions, self-made nitrogen filling equipment was used to SI/R in the cells of this experiment. Thirdly, we used the MROS assay kit from Cayman in our measurement of MROS. However, the relevant literature displayed on the official website does not include any records of the kit's usage, only the principles related to the kit are presented. The reviewer believes that this may lead to insufficient credibility of the results. Nonetheless, there are reliable studies that utilize this principle for MROS detection. I believe the reviewer's opinion is valuable, and more research is indeed needed to validate the effectiveness of this kit⁴⁴. Finally, In the SI/R environment, the regulatory mechanism of cells is very complex. In this experiment, it was observed that after SI/R treatment, the O-GlcNAcylation level of SIRT3 was upregulated, but the activity was reduced, This experiment did not conduct in-depth mechanism research on this phenomenon.

Fundings

This work was supported by the First Affiliated Hospital of Harbin Medical University [Grant Nos. 2020IIT047 to J.J.L., Grant Nos. 2023IIT129 to L.S.].

Data availability

All data generated or analysed during this study are included in this published article [and its supplementary information files].

Received: 4 April 2024; Accepted: 5 September 2024

Published online: 11 September 2024

References

- Anderson, J. L. & Morrow, D. A. Acute myocardial infarction. *N. Engl. J. Med.* **376**, 2053–2064 (2017).
- Cung, T.-T. *et al.* Cyclosporine before PCI in patients with acute myocardial infarction. *N. Engl. J. Med.* **373**, 1021–1031 (2015).
- Cabrera-Fuentes, H. A. *et al.* From basic mechanisms to clinical applications in heart protection, new players in cardiovascular diseases and cardiac theranostics: Meeting report from the third international symposium on “New frontiers in cardiovascular research”. *Basic Res. Cardiol.* **111**, 69 (2016).
- Ibáñez, B., Heusch, G., Ovize, M. & Van de Werf, F. Evolving therapies for myocardial ischemia/reperfusion injury. *J. Am. Coll. Cardiol.* **65**, 1454–1471 (2015).
- Fröhlich, G. M., Meier, P., White, S. K., Yellon, D. M. & Hausenloy, D. J. Myocardial reperfusion injury: Looking beyond primary PCI. *Eur. Heart J.* **34**, 1714–1722 (2013).
- Davidson, S. M. *et al.* Multitarget strategies to reduce myocardial ischemia/reperfusion injury: JACC review topic of the week. *J. Am. Coll. Cardiol.* **73**, 89–99 (2019).
- Heusch, G. Critical issues for the translation of cardioprotection. *Circ. Res.* **120**, 1477–1486 (2017).
- Shi, B., Ma, M., Zheng, Y., Pan, Y. & Lin, X. mTOR and Beclin1: Two key autophagy-related molecules and their roles in myocardial ischemia/reperfusion injury. *J. Cell Physiol.* **234**, 12562–12568 (2019).
- Daniels, L. J. *et al.* Myocardial energy stress, autophagy induction, and cardiomyocyte functional responses. *Antioxid. Redox Signal* **31**, 472–486 (2019).
- Petrovski, G. *et al.* Cardioprotection by endoplasmic reticulum stress-induced autophagy. *Antioxid. Redox Signal* **14**, 2191–2200 (2011).
- Loos, B., Genade, S., Ellis, B., Lochner, A. & Engelbrecht, A. M. At the core of survival: Autophagy delays the onset of both apoptotic and necrotic cell death in a model of ischemic cell injury. *Exp. Cell Res.* **317**, 1437–1453 (2011).

12. Matsui, Y. *et al.* Distinct roles of autophagy in the heart during ischemia and reperfusion: Roles of AMP-activated protein kinase and Beclin 1 in mediating autophagy. *Circ. Res.* **100**, 914–922 (2007).
13. Chen, Y.-R. & Zweier, J. L. Cardiac mitochondria and reactive oxygen species generation. *Circ. Res.* **114**, 524–537 (2014).
14. Chen, W. R. *et al.* Melatonin attenuates myocardial ischemia/reperfusion injury by inhibiting autophagy via an AMPK/mTOR signaling pathway. *Cell Physiol. Biochem.* **47**, 2067–2076 (2018).
15. Lee, H.-L., Chen, C.-L., Yeh, S. T., Zweier, J. L. & Chen, Y.-R. Biphasic modulation of the mitochondrial electron transport chain in myocardial ischemia and reperfusion. *Am. J. Physiol. Heart Circ. Physiol.* **302**, H1410–H1422 (2012).
16. Paradies, G. *et al.* Decrease in mitochondrial complex I activity in ischemic/reperfused rat heart: Involvement of reactive oxygen species and cardiolipin. *Circ. Res.* **94**, 53–59 (2004).
17. Scherz-Shouval, R. & Elazar, Z. Regulation of autophagy by ROS: Physiology and pathology. *Trends Biochem. Sci.* **36**, 30–38 (2011).
18. Schiattarella, G. G. & Hill, J. A. Metabolic control and oxidative stress in pathological cardiac remodelling. *Eur. Heart J.* **38**, 1399–1401 (2017).
19. Dikalova, A. E. *et al.* Sirt3 impairment and SOD2 hyperacetylation in vascular oxidative stress and hypertension. *Circ. Res.* **121**, 564–574 (2017).
20. Qiu, X., Brown, K., Hirschey, M. D., Verdin, E. & Chen, D. Calorie restriction reduces oxidative stress by SIRT3-mediated SOD2 activation. *Cell Metab.* **12**, 662–667 (2010).
21. Ma, L.-L. *et al.* Hypertrophic preconditioning attenuates myocardial ischaemia-reperfusion injury by modulating SIRT3-SOD2-mROS-dependent autophagy. *Cell Prolif.* **54**, e13051 (2021).
22. Pillai, V. B. *et al.* Exogenous NAD blocks cardiac hypertrophic response via activation of the SIRT3-LKB1-AMP-activated kinase pathway. *J. Biol. Chem.* **285**, 3133–3144 (2010).
23. Chatham, J. C., Zhang, J. & Wende, A. R. Role of O-linked N-acetylglucosamine protein modification in cellular (Patho)physiology. *Physiol. Rev.* **101**, 427–493 (2021).
24. Torres, C. R. & Hart, G. W. Topography and polypeptide distribution of terminal N-acetylglucosamine residues on the surfaces of intact lymphocytes. Evidence for O-linked GlcNAc. *J. Biol. Chem.* **259**, 3308–3317 (1984).
25. Yang, X. & Qian, K. Protein O-GlcNAcylation: Emerging mechanisms and functions. *Nat. Rev. Mol. Cell Biol.* **18**, 452–465 (2017).
26. Zachara, N. E. *et al.* Dynamic O-GlcNAc modification of nucleocytoplasmic proteins in response to stress. A survival response of mammalian cells. *J Biol Chem* **279**, 30133–30142 (2004).
27. Vibjerg Jensen, R., Johnsen, J., Buus Kristiansen, S., Zachara, N. E. & Bøtker, H. E. Ischemic preconditioning increases myocardial O-GlcNAc glycosylation. *Scand. Cardiovasc. J.* **47**, 168–174 (2013).
28. Jensen, R. V. *et al.* Impact of O-GlcNAc on cardioprotection by remote ischaemic preconditioning in non-diabetic and diabetic patients. *Cardiovasc. Res.* **97**, 369–378 (2013).
29. Champattanachai, V., Marchase, R. B. & Chatham, J. C. Glucosamine protects neonatal cardiomyocytes from ischemia-reperfusion injury via increased protein-associated O-GlcNAc. *Am. J. Physiol. Cell Physiol.* **292**, C178–C187 (2007).
30. Han, C. *et al.* O-GlcNAcylation of SIRT1 enhances its deacetylase activity and promotes cytoprotection under stress. *Nat. Commun.* **8**, 1491 (2017).
31. He, X. *et al.* O-GlcNAcylation and stabilization of SIRT7 promote pancreatic cancer progression by blocking the SIRT7-REGY interaction. *Cell Death Differ.* **29**, 1970–1981 (2022).
32. Sun, L. *et al.* Salidroside and tyrosol from *Rhodiola* protect H9c2 cells from ischemia/reperfusion-induced apoptosis. *Life Sci.* **91**, 151–158 (2012).
33. Lavu, S., Boss, O., Elliott, P. J. & Lambert, P. D. Sirtuins—novel therapeutic targets to treat age-associated diseases. *Nat. Rev. Drug Discov.* **7**, 841–853 (2008).
34. Zhang, J. *et al.* Mitochondrial Sirtuin 3: New emerging biological function and therapeutic target. *Theranostics* **10**, 8315–8342 (2020).
35. Liu, R. *et al.* CDK1-mediated SIRT3 activation enhances mitochondrial function and tumor radioresistance. *Mol. Cancer Ther.* **14**, 2090–2102 (2015).
36. Wang, T. *et al.* SENP1-Sirt3 signaling controls mitochondrial protein acetylation and metabolism. *Mol. Cell* **75**, 823 (2019).
37. Marsh, S. A., Collins, H. E. & Chatham, J. C. Protein O-GlcNAcylation and cardiovascular (patho)physiology. *J. Biol. Chem.* **289**, 34449–34456 (2014).
38. Imai, S., Armstrong, C. M., Kaeberlein, M. & Guarente, L. Transcriptional silencing and longevity protein Sir2 is an NAD-dependent histone deacetylase. *Nature* **403**, 795–800 (2000).
39. He, H., Liu, P. & Li, P. Dexmedetomidine ameliorates cardiac ischemia/reperfusion injury by enhancing autophagy through activation of the AMPK/SIRT3 pathway. *Drug Des. Dev. Ther.* **17**, 3205–3218 (2023).
40. Wu, J., Yang, Y., Gao, Y., Wang, Z. & Ma, J. Melatonin attenuates anoxia/reoxygenation injury by inhibiting excessive mitophagy through the MT2/SIRT3/FoxO3a signaling pathway in H9c2 cells. *Drug Des. Dev. Ther.* **14**, 2047–2060 (2020).
41. Ngoh, G. A., Watson, L. J., Facundo, H. T. & Jones, S. P. Augmented O-GlcNAc signaling attenuates oxidative stress and calcium overload in cardiomyocytes. *Amino Acids* **40**, 895–911 (2011).
42. Jones, S. P. *et al.* Cardioprotection by N-acetylglucosamine linkage to cellular proteins. *Circulation* **117**, 1172–1182 (2008).
43. Jang, I. *et al.* O-GlcNAcylation of eIF2 α regulates the phospho-eIF2 α -mediated ER stress response. *Biochim. Biophys. Acta* **1853**, 1860–1869 (2015).
44. Pi, H. *et al.* SIRT3-SOD2-mROS-dependent autophagy in cadmium-induced hepatotoxicity and salvage by melatonin. *Autophagy* **11**, 1037–1051 (2015).

Acknowledgements

We thank Institute of Cardiology, the First Clinical College of Harbin Medical University.

Author contributions

H.Z.: Idea conceptualization, data collection, data processing and analysis, creation of graphs and tables, initial manuscript drafting, final approval for publication. Y.J.: Idea conceptualization, data processing and analysis, creation of graphs and tables, initial manuscript drafting, final approval for publication. L.S.: Data selection, data analysis, initial manuscript drafting, final approval for publication, funding, project administration. J.L.: Data selection, data analysis, initial manuscript drafting, final approval for publication, funding, project administration, Supervision.

Competing interests

The authors declare no competing interests.

Additional information

Supplementary Information The online version contains supplementary material available at <https://doi.org/10.1038/s41598-024-72324-z>.

Correspondence and requests for materials should be addressed to J.L. or L.S.

Reprints and permissions information is available at www.nature.com/reprints.

Publisher's note Springer Nature remains neutral with regard to jurisdictional claims in published maps and institutional affiliations.

Open Access This article is licensed under a Creative Commons Attribution-NonCommercial-NoDerivatives 4.0 International License, which permits any non-commercial use, sharing, distribution and reproduction in any medium or format, as long as you give appropriate credit to the original author(s) and the source, provide a link to the Creative Commons licence, and indicate if you modified the licensed material. You do not have permission under this licence to share adapted material derived from this article or parts of it. The images or other third party material in this article are included in the article's Creative Commons licence, unless indicated otherwise in a credit line to the material. If material is not included in the article's Creative Commons licence and your intended use is not permitted by statutory regulation or exceeds the permitted use, you will need to obtain permission directly from the copyright holder. To view a copy of this licence, visit <http://creativecommons.org/licenses/by-nc-nd/4.0/>.

© The Author(s) 2024